Photocurrent of hydrogenated nanocrystalline silicon thin film/crystalline silicon heterostructure

R. Zhang,[a] X. Y. Chen, J. J. Lu, and W. Z. Shen[b]
Laboratory of Condensed Matter Spectroscopy and Opto-Electronic Physics, Department of Physics, Shanghai Jiao Tong University, 1954 Hua Shan Road, Shanghai 200030, China

(Received 26 August 2007; accepted 24 October 2007; published online 27 December 2007)

We report on the photocurrent properties of the hydrogenated nanocrystalline silicon (nc-Si:H) thin film/crystalline silicon (c-Si) *n-p* heterostructure. By comparison with the c-Si *n-p* homojunction, two Gaussian-type photocurrent peaks are observed in the nc-Si:H/c-Si heterostructure and attributed to be transitions from a tail band or discrete levels in quantum dots with localized states, and a miniband with extended states associated with the embedded nanometer crystallites in the amorphous boundaries of the nc-Si:H thin film. The observed strong photocurrent signals and temperature dependency have revealed the unique electronic states of the miniband in the nc-Si:H thin film. Our investigations into the photocurrent properties may help to realize nc-Si:H/c-Si heterostructure-based optoelectronic devices. © *2007 American Institute of Physics*.
[DOI: 10.1063/1.2826742]

I. INTRODUCTION

Hydrogenated nanocrystalline silicon (nc-Si:H) thin films have attracted considerable interest due to their importance in fundamental physics and potential applications to optoelectronic devices such as light-emitting diodes,[1] optical memories,[2] solar cells,[3] thin-film transistors,[4] and single-electron transistors.[5] The nc-Si:H thin film has the advantages of both high stability under light[6] and high electron-hole generation rate with respect to amorphous silicon (a-Si) alloy, where the photocurrent is dominated by the electron transitions due to the hole capture by the intrinsic defects, especially the metastable Staebler-Wronski-related defects.[7] Unlike the a-Si material, the exciton state of the bounded electron-hole pair in grains of the nc-Si:H thin film can be formed by the absorption of the photon, and easily separated to be the free-photogenerated carrier under the electric field due to the relatively ordered structure of nc-Si:H thin film.[8] In addition, the high-density nanometer grains and voids effectively enhance the optical absorption cross section in the nc-Si:H thin film, resulting in the high optical absorption and photocurrent in the hydrogenated microcrystalline Si (μc-Si:H) or nc-Si:H thin film with high crystalline volume fraction.[6,9]

Recently, we have realized highly ordered nc-Si:H thin films (where Si nanocrystals are embedded in a-Si:H networks) on lattice-matched c-Si substrates under optimized growth conditions by plasma-enhanced chemical vapor deposition (PECVD), and reported the corresponding high room-temperature electron mobility and dark conductivity of the nc-Si:H films on the order of 10^2 cm^2/Vs and 10^1 S cm^{-1}, respectively.[10] Moreover, the visible photoluminescence (PL) has also been observed.[11] The improved electron mobility and conductivity of the nc-Si:H thin films would be advantageous to the photogenerated carrier collection, leading to a wide range of optoelectronic applications with higher performances, such as the infrared detection and imaging devices.[12,13] On the foundation of these improvements, it is possible for the high-speed electronic transport circuit and visible luminescence, as well as the electrical-optical conversion, to be integrated on a single chip by the nc-Si:H thin film.

In this paper, we employ the photocurrent spectroscopy for investigations on the optoelectronic characteristics of the highly ordered nc-Si:H thin film with a heterostructure grown on the c-Si substrate, together with the comparison study of a c-Si *n-p* homojunction. The temperature- and bias-voltage-dependent photocurrent spectra of the nc-Si:H thin film reveal rich information of the electronic transition in the highly ordered nc-Si:H thin film.

II. EXPERIMENTAL DETAILS

The nc-Si:H thin film/c-Si heterostructure sample was prepared in a radio frequency (13.56 MHz and power 75 W) capacitive coupled PECVD system from silane (SiH_4) and hydrogen (H_2) at a temperature of 250 °C and chamber pressure of 1.0 Torr. The percentage content of silane (SiH_4/SiH_4+H_2) was about 1.0%. The nc-Si:H thin film samples with thickness of ~1.0 μm were doped with phosphine (PH_3/SiH_4) of ~0.8% on the *p*-type silicon substrates. The structure of the nc-Si:H film had been characterized by the x-ray diffraction and Raman scattering measurements, as reported in Ref. 10. It was shown that the studied nc-Si:H sample with crystalline volume fraction $X_C \sim 52\%$ consists of the highly dense Si grains (10nm or less in size) separated by very narrow a-Si:H boundaries (about 2–4 atomic spacing in thickness).

The photocurrent measurements were carried out on a Nicolet Nexus 870 Fourier transform infrared (FTIR) spectrometer calibrated by a DTGS TEC detector. Two electrodes

[a]Also at Division of Basic Courses, Shanghai Maritime University, Shanghai 200135, China.
[b]Author to whom correspondence should be addressed. Electronic mail: wzshen@sjtu.edu.cn.

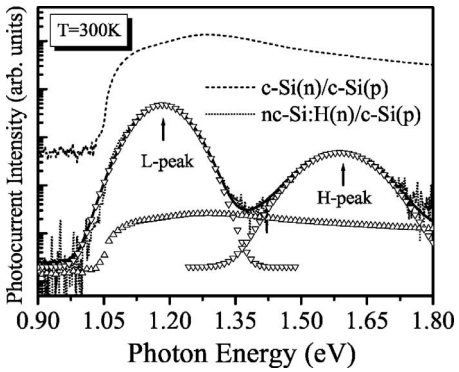

FIG. 1. Room-temperature experimental photocurrent spectra of the nc-Si:H(n)/c-Si(p) heterostructure (dotted curve) and a typical c-Si(n)/c-Si(p) homojunction (dashed curve) for comparison.

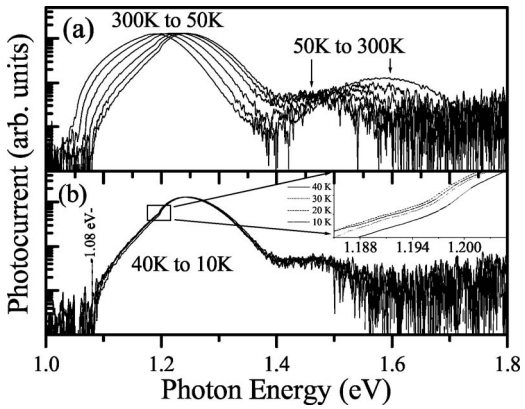

FIG. 2. Photocurrent spectra of the nc-Si:H/c-Si heterostructure with temperature decreasing from (a) 300 to 50 K and (b) 40 to 10 K. The inset shows the magnified variations of the photocurrent at temperatures below 50 K.

were fabricated on both sides of the studied nc-Si:H(n)/c-Si(p) heterostructure diode. By using a Keithley 2400 source meter, a dc bias voltage was applied to the sample to modulate its built-in potential. In addition, temperature-dependent photocurrent spectra had been measured by placing the samples in an Oxford optical cryostat, and the temperature range was set from 300 to 8 K.

III. RESULTS AND DISCUSSION

Figure 1 presents the room-temperature experimental photocurrent spectrum of the studied nc-Si:H(n)/c-Si(p) heterostructure under zero bias voltage by the dotted curve, together with the corresponding result of a typical c-Si(n)/c-Si(p) homojunction by the dashed curve for comparison. Two distinct peaks above the photon energy of the c-Si band gap 1.08 eV are clearly observed in the photocurrent spectrum of the nc-Si:H(n)/c-Si(p) heterostructure sample. This double-peak feature is quite different from the broad photocurrent peak of the counterpart c-Si(n)/c-Si(p) homojunction sample. Generally, the photocurrent generated in the c-Si material increases with the photon energy at the low-energy side of the band gap due to the increase of the photon absorption. Once the photon energy is beyond the band-gap energy, the strong optical absorption will increase not only the excessive carrier density, but also the recombination rate, especially on the thin-film surface. Therefore, the photocurrent of the c-Si(n)/c-Si(p) homojunction shows a typical broad structure above the band gap and a small drop in the high-absorption region.

On the other hand, for the nc-Si:H(n)/c-Si(p) heterostructure sample, the photocurrent spectrum is obviously dominated by two Gaussian-shaped peaks on a broad background, as shown in Fig. 1. The broad background photocurrent starts from photon energy close to the band gap of Si, and it is very small in amplitude compared with the two Gaussian-shaped peaks. We can reasonably assign the origin of the weak background photocurrent to the c-Si substrate, since the incident light to the substrate has been weakened after the absorption of the 1 μm thickness nc-Si:H thin film. Assuming that the photocurrent from the c-Si substrate appears with the same broad structure as that of the c-Si(n)/c-Si(p) homojunction, we can decompose the photocurrent of the nc-Si:H(n)/c-Si(p) heterostructure sample into two Gaussian-shaped peaks (denoted by antitriangle scatters) and a broad background photocurrent (denoted by triangle scatters). The solid curve is the calculated result considering the total contributions from both the parts, which fit very well with the experimental photocurrent of the nc-Si:H(n)/c-Si(p) heterostructure sample (dotted curve). The two Gaussian-shaped photocurrent peaks occur at the photon energy below and above ~1.4 eV, as denoted by the *L*-peak and *H*-peak, respectively. Their amplitudes are 10–100 times larger than the broad background photocurrent from the c-Si substrate. Moreover, they show quite different behaviors of photon energy and temperature dependencies from the photocurrent spectra of c-Si, which will be discussed below. As a result, the two Gaussian-shaped photocurrent peaks can be considered to be originated from the nc-Si:H thin film.

Figure 2 shows the photocurrent spectra of the studied nc-Si:H(n)/c-Si(p) sample for temperature (a) above 50 K and (b) below 50 K. These two Gaussian-shaped peaks show quite different temperature-dependent behaviors above 50 K, but are almost temperature independent below 50 K. For the *H*-peak, it demonstrates a strong temperature dependency above 50 K, i.e., a thermal activation behavior. Furthermore, its photon energy position is ~1.6 eV at room temperature, far above the band-gap energy of c-Si, but consistent with many spectra previously reported for a-Si:H.[7] Therefore, this *H*-peak photocurrent can be easily attributed to the electronic transitions from the tail band of a-Si boundaries in nc-Si:H, where the photoexcited carriers transport in a thermally activated hopping behavior. With the temperature decreasing, the thermally activated *H*-peak photocurrent is partially quenched for photon energy above ~1.6 eV, as shown in Fig. 2(a). For the temperature below 50 K, the *H*-peak shifts toward the low photon energy side and turns out to be a temperature-independent steplike structure [see Fig. 2(b)]. This kind of temperature-independent behavior clearly reveals the tunneling transport of the photoexcited carriers, which are the transitions from the discrete levels of the nanometer grains embedded in the a-Si:H boundaries. It is the misalignment of these discrete levels in energy due to the

grain size distribution that causes the *H*-peak photocurrent to quench with the decreasing temperature and become a temperature-independent steplike structure, together with observable unstable fluctuations for photon energy above ~1.6 eV below 50 K. In addition, the recombination of excitons confined in these quantum weak localized states (or discrete levels of nanometer grains) has been demonstrated by PL at the same photon energy,[14] and observed for the studied sample in Ref. 11. The photocurrent and PL at such photon energies above the c-Si band gap have also been reported in the μc-Si:H thin film,[15] a-Si:H/c-Si,[13] porous Si/c-Si,[16] and μc-Si:H/c-Si (Ref. 8) heterostructures.

For the *L*-peak photocurrent centering at about ~1.2 eV, it begins with the threshold photon energy of 1.05 eV and increases beyond 2 orders of magnitude to its maximum. It seems that this *L*-peak photocurrent is mainly contributed by the photoexcited carriers generated in the c-Si substrate, in view of the same threshold photon energy 1.05 eV comparing with the c-Si(n)/c-Si(p) sample in Fig. 1. However, this assumption has been excluded by the special photon energy dependency in the photocurrent spectrum described above, and the temperature dependency of the experimental photocurrent results, which will further help us to identify the origin of the *L*-peak.

In Fig. 2(a), a shift to higher photon energy and nondegradation of the *L*-peak with decreasing temperature from 300 to 50 K has been clearly observed. Furthermore, it reveals a two-component phenomenon in the photocurrent at temperature below 50 K, where the distinct double threshold of the spectra occurs at the photon energy of ~1.08 and ~1.20 eV, respectively [see the enlarged part in the inset of Fig. 2(b)]. A similar two-component nature also appears in the photocurrent of c-Si at a low temperature of 4 K with the double-threshold photon energy at 1.14 and 1.19 eV, and the photon energy difference is caused by the absorption enhancement of the optical phonon with a energy of ~50 meV [Fig. 12 of Ref. 17]. It should be noted that the photon energy difference in the two-component nature of the studied nc-Si:H(n)/c-Si(p) sample is about 110 meV, which is much larger than the optical phonon energy in Si. Therefore, it is impossible for the well-defined onset photocurrent at 1.2 eV in the nc-Si:H(n)/c-Si(p) sample to be induced by the optical phonons; they are caused by the formation of a discrete level in the nc-Si:H thin film and band discontinuity at the nc-Si:H(n)/c-Si(p) interface below 50 K, which has been demonstrated by the electron resonant tunneling phenomenon in Ref. 10. A similar increase of photocurrent above the band-gap energy has also been observed in the GaAs homojunction system with a thin silicon interlayer buried (p-GaAs/δSi/n-GaAs) due to the artificial band discontinuity.[18] In addition, the formation of the discrete level is accompanied by an abnormal increase in the photocurrents at the band edge with the temperature decreasing below 50 K, as shown in the inset of Fig. 2. These special temperature-dependent behaviors of the *L*-peak photocurrent further clarify that it originates from the photoexcited carriers generated in the nc-Si:H thin film, rather than the c-Si substrate. However, the *L*-peak photocurrent below the threshold of 1.2 eV also takes on some typical behaviors similar to those of the c-Si, as discussed below.

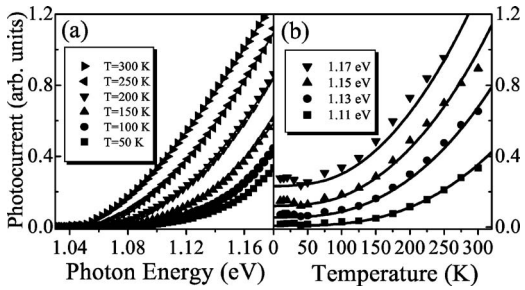

FIG. 3. (a) *L*-peak photocurrent spectra on low-energy side for temperature ranging from 300 to 50 K and (b) temperature-dependent photocurrent at the photon energy ranging from 1.17 to 1.11 eV for temperature from 300 to 10 K. Scatters are experimental results and solid curves are theoretical results.

Figure 3(a) displays the *L*-peak photocurrent spectra at the low-energy side for temperature ranging from 300 to 50 K and (b) plots the photocurrent as a function of temperature for the photon energy ranging from 1.17 to 1.11 eV. It should be noted that an increase of the onset photocurrent in the *L*-peak with the temperature is clearly observed in Fig. 3(a), similar to the temperature-dependent absorption edge of the c-Si material.[19] This normal increase in the experimental photocurrent of the nc-Si:H thin film clearly demonstrates that the optical absorption is assisted by the phonons, where the phonon-assisted absorption contributes to the photocurrent at the temperature above 50 K. Usually, the photocurrent near the band edge due to the phonon-assisted absorption in the indirect band gap system follows the classical power function of the photon energy

$$I_{\mathrm{PC}}(\hbar\omega) \propto (\hbar\omega - E_g)^x, \tag{1}$$

with the power number $x=2$ ($x=1/2$ indicates the transition in the direct band-gap system). Above 50 K, the onset of *L*-peak photocurrents in the studied sample are all well fitted by the above equation with x in the range of 1.5–2.3, as revealed by the good agreement between the experimental scatters and calculated curves in Fig. 3(a). The obtained power number x is close to 2, indicating the phonon-assisted transition nature of the *L*-peak photocurrent, similar to that in the c-Si.

For the phonon-assisted transition absorption, the optical absorption can be expressed by[20]

$$\alpha \propto \frac{(\hbar\omega - E_g - E_p)^2}{1 - \exp(-E_p/k_B T)} + \frac{(\hbar\omega - E_g + E_p)^2}{\exp(E_p/k_B T) - 1}, \tag{2}$$

with optical-absorption coefficient α, photon energy $\hbar\omega$, Boltzmann constant k_B, phonon energy E_p, and band-gap energy E_g. In the weak absorption regime near the band edge, the photocurrent is directly proportional to the strength of optical absorption.[9] This classical equation can well describe the variation of the photocurrent versus temperature, as shown by the good agreement between the scatters and solid curves calculated by Eq. (2) in Fig. 3(b). The obtained photon energy E_p, ranging from 33 to 49 meV, is well in the range of phonon energy of Si. The successful explanation of the photocurrent from the nc-Si:H thin film by the classical Eq. (2) due to the phonon-assisted transition indicates that

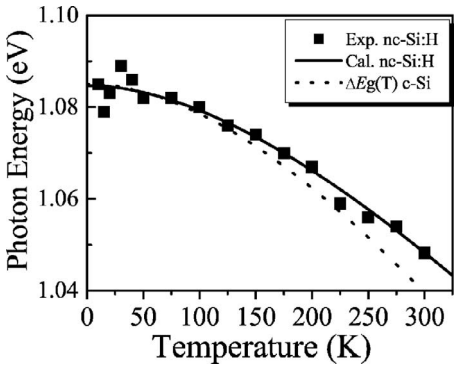

FIG. 4. Miniband gap energy of the nc-Si:H thin film as a function of temperature by square scatters, and fitted results by solid curve, together with the temperature-dependent band-gap variation $[\Delta E_g(T)=E_g(T)-E_0$, in which E_0 is a constant energy of 55 meV] of c-Si by the dotted curve.

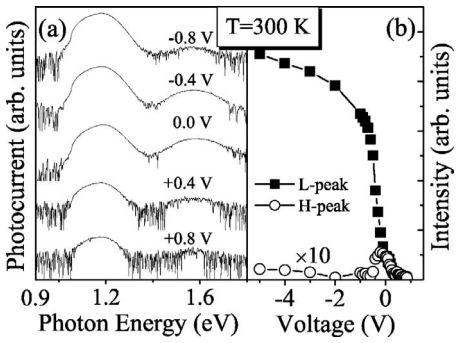

FIG. 5. Bias voltage-dependent (a) photocurrent spectra and (b) photocurrent intensity of the *L*-peak (1.2 eV) and *H*-peak (1.6 eV, with a multiplying factor of 10) at room temperature.

the energy band of the continuous states is also formed in the nc-Si:H thin film like that in c-Si. It should be noted that the *L*-peak photocurrent from the transitions of the Si-like continuous energy band is very narrow in terms of the energy width (~300 meV at half height of the *L*-peak), and it is quite larger than the phonon energy of nc-Si:H thin film, which means a miniband. It is the high density of nanometer grains embedded in the very thin a-Si:H boundaries that results in a superposition of a miniband with a Si-like band gap in the tail band of a-Si:H in the nc-Si:H.

In Fig. 3(b), a discrepancy between the scatters and solid curves can be observed that increases with the photon energy, because the condition of $I_{PC} \propto \alpha$ becomes invalid with the increase of the optical absorption. In addition, at the band-gap edge, the deviation between the scatters and solid curves becomes much clearer with the temperature decreasing below 50 K, where an abnormal increase of photocurrent is clearly revealed. This abnormal phenomenon demonstrates that the photocurrent of the nc-Si:H thin film at band edge is not contributed from the phonon-assisted transition mechanism described by Eq. (2), but from the transition of the quantum discrete level in the continuous energy band of the nc-Si:H thin film below 50 K. Furthermore, the formation of the quantum discrete level in the miniband causes not only the abnormal photocurrent at the band edge below 50 K, but also another threshold in the photocurrent above the band gap, as demonstrated in the inset of Fig. 2(b).

Figure 4 lists the miniband gap versus temperature by the scatters, which is extracted from the fitting results of the threshold in the photocurrent spectra. The band-gap energy of the nc-Si:H thin film decreases with the temperature and can be fitted well by the classical Varshni equation,[21]

$$E_g(T) = E_g^0 - \frac{AT^2}{B+T}, \tag{3}$$

with constants $A=3.2\times10^{-4}$, $B=490.5$ K, and $E_g^0=1.085$ eV. It is clear that the temperature dependency of the band gap of the nc-Si:H thin film (solid curve) is very close to that of the c-Si (dotted curve), which is calculated by $\Delta E_g(T)=E_g(T)-E_0$ with $E_g(T)$ given in Ref. 21 and an energy shift of $E_0=55$ meV. As mentioned above, the miniband in the nc-Si:H thin film has many similarities to the continuous energy band of c-Si: indirect transition, band-gap energy, and its temperature dependency. These similarities between the nanometer grain system and c-Si strongly depend on the extremely thin a*a*-Si:H boundaries and highly ordered structure, which is grown under the condition of the a-Si substrate and hydrogenation-induced ordered structure.[10]

Although the above temperature-dependent *L*-peak photocurrent exhibits the same continuous states in the nc-Si:H thin film as those in the c-Si, the energy band of the nc-Si:H thin film is quite different from that of c-Si and contains a miniband beginning from the c-Si band gap to the energy of ~1.4 eV, together with a tail band and discrete levels above ~1.4 eV. It is this miniband that causes the Gaussian-type *L*-peak photocurrent ranging from the band gap to 1.4 eV in Fig. 2. Moreover, a discrete level at 1.2 eV will be formed in the miniband at the temperature below 50 K, as evidenced by the two-component nature of the *L*-peak in Fig. 2(b). Above the photon energy of 1.4 eV, it is the transition from band tail states or the discrete levels that leads to the *H*-peak photocurrent. For the photoexcited carriers generated by the tail band or discrete levels above the photon energy of 1.4 eV, the mobility is very small, which is because their thermal-assisted hopping transportation results from the energy distribution of discrete levels on the nearest hopping sites. In addition, the quantum confined effect of the photoexcited carriers generated by the band tail or discrete levels also brings a strong recombination over the escape process, which causes an increase of the intensity of PL signals[11] and a reduction of the photocurrent intensity.[22] Therefore, the *H*-peak photocurrent contributed by transitions from band tail states or discrete levels is much lower than the *L*-peak one due to the continuous states in the miniband, as a result of the high recombination and low mobility of the photoexcited carriers.

Figure 5 presents the room-temperature bias voltage-dependent (a) photocurrent spectra and (b) photocurrent intensity of the *L*-peak (at 1.2 eV) and *H*-peak (at 1.6 eV). It is clear that the photocurrent intensity of the nc-Si:H/c-Si heterostructure is sensitive to the external bias voltage. However, the intensities of the two photocurrent peaks take on different bias voltage-dependent behaviors, as shown by the squares for the *L*-peak and circles for the *H*-peak in Fig. 5(b). For the *L*-peak, the photocurrent increases rapidly with

the voltage decreasing into the reversed bias region. The negative bias boosts the *L*-peak photocurrent more than 2 orders of magnitude due to an increased depletion width in the heterostructure under reverse bias.[23] For the *H*-peak, it becomes weak and displays strong fluctuations on both the positive and negative bias in Fig. 5(a), indicating the discrete levels unaligned in energy or instability of the tail states due to the external electrical field.

IV. CONCLUSIONS

The highly ordered nc-Si:H thin film grown on c-Si substrate has been revealed to be a system of electronic states, including a miniband with a Si-like band gap embedded in a tail band of a-Si:H boundaries. We have experimentally demonstrated two Gaussian-type peaks in the photocurrent spectra, which are contributed from the miniband and tail band at temperature above 50 K. Below 50 K, a quantum discrete level can be formed in the miniband, leading to an abnormal increase in the photocurrent at the band edge of the miniband. It is the continuous electronic states in the miniband where the high and non-reduction photocurrent can be achieved at low temperatures. Furthermore, the photocurrent response can be further enhanced by the reverse bias voltage through construction of the nc-Si:H/c-Si heterostructure.

ACKNOWLEDGMENTS

This work was supported by the National Natural Science Foundation of China under Contract Nos. 10674094 and 10734020, the National Major Basic Research Project No. 2006CB921507, the National Ministy of Education Program for Changjiang Scholars and Innovative Research Team in University, No. IRT0524, and Shanghai Municipal Commission of Science and Technology, Project Nos. 05DJ14003 and 06JC14039, as well as the Excellent Young Teacher Plan, No. 025063, at Shanghai Maritime University.

[1] A. G. Cullis, L. T. Canham, and P. D. J. Calcott, J. Appl. Phys. **82**, 909 (1997).
[2] R. J. Walters, P. G. Kik, J. D. Casperson, H. A. Atwater, R. Lindstedt, M. Giorgi, and G. Bourianoff, Appl. Phys. Lett. **85**, 2622 (2004).
[3] A. Shah, P. Torres, R. Tscharner, N. Wyrsch, and H. Keppner, Science **285**, 692 (1999); I. C. Cheng and S. Wagner, Appl. Phys. Lett. **80**, 440 (2002).
[4] B. Kalache, A. I. Kosarev, R. Vanderhaghen, and P. Roca i Cabarrocas, J. Appl. Phys. **93**, 1262 (2003).
[5] Y. T. Tan, T. Kamiya, Z. A. K. Durrani, and H. Ahmed, Appl. Phys. Lett. **78**, 1083 (2001).
[6] D. V. Tsu, B. S. Chao, S. R. Ovshinsky, S. Guha, and J. Yang, Appl. Phys. Lett. **71**, 1317 (1997).
[7] A. V. Gelatos, K. K. Mahavadi, J. D. Cohen, and J. P. Harbison, Appl. Phys. Lett. **53**, 403 (1988).
[8] D. Kwon, C. C. Chen, J. D. Cohen, H. C. Jin, E. Hollar, I. Robertson, and J. R. Abelson, Phys. Rev. B **60**, 4442 (1999).
[9] R. Zhang, X. Y. Chen, K. Zhang, and W. Z. Shen, J. Appl. Phys. **100**, 104310 (2006).
[10] X. Y. Chen, W. Z. Shen, and Y. L. He, J. Appl. Phys. **97**, 024305 (2005); X. Y. Chen and W. Z. Shen, Phys. Rev. B **72**, 035309 (2005); X. Y. Chen and W. Z. Shen, Appl. Phys. Lett. **85**, 287 (2004).
[11] H. Chen, W. Z. Shen, and W. S. Wei, Appl. Phys. Lett. **88**, 121921 (2006).
[12] M. Tucci and R. DeRosa, Solid-State Electron. **44**, 1315 (2000).
[13] H. Mimura and Y. Hatanaka, J. Appl. Phys. **61**, 2575 (1987).
[14] S. Takeoka, M. Fujii, and S. Hayashi, Phys. Rev. B **62**, 16820 (2000).
[15] M. N. Islam and S. Kumar, J. Appl. Phys. **93**, 1753 (2003).
[16] H. T. Shi, Y. D. Zheng, Y. B. Wang, and R. K. Yuan, Appl. Phys. Lett. **63**, 770 (1993).
[17] T. P. Pearsall, L. Colace, D. V. Adam, W. Jäger, D. Stenkamp, G. Theodorou, H. Presting, E. Kasper, and K. Thonke, Phys. Rev. B **57**, 9128 (1998).
[18] T. dell'Orto, J. Almeida, C. Coluzza, A. Baldereschi, T. Margaritondo, M. Cantile, S. Yildirim, L. Sorba, and A. Franciosi, Appl. Phys. Lett. **64**, 2111 (1994).
[19] G. G. Macfarlane, T. P. Mclean, J. E. Quarrington, and V. Roberts, Phys. Rev. **111**, 1245 (1958).
[20] S. C. Shen, *Spectroscopy and Optical Properties of Semiconductors* (Scientific Press, Beijing, 2002), p. 58.
[21] G. E. Jellison, Jr. and D. H. Lowndes, Appl. Phys. Lett. **41**, 594 (1982).
[22] P. N. Brunkov, A. Patane, A. Levin, L. Eaves, P. C. Main, Y. G. Musikhin, B. V. Volovik, A. E. Zhukov, V. M. Ustinov, and S. G. Konnikov, Phys. Rev. B **65**, 085326 (2002).
[23] R. S. Crandall, R. Williams, and B. Tompkins, J. Appl. Phys. **50**, 5506 (1979).